AMERICAN SOCIETY FOR MICROBIOLOGY | mBio®

OBSERVATION

Candida albicans Filamentation Does Not Require the cAMP-PKA Pathway *In Vivo*

Rohan S. Wakade,[a] Juraj Kramara,[a] Melanie Wellington,[a] Damian J. Krysan[a,b]

[a]Department of Pediatrics, Carver College of Medicine, University of Iowa, Iowa City, Iowa, USA
[b]Department of Microbiology and Immunology, Carver College of Medicine, University of Iowa, Iowa City, Iowa, USA

ABSTRACT *Candida albicans* is one of the most prevalent human fungal pathogens. Its ability to transition between budding yeast and filamentous morphological forms (pseudohyphae and hyphae) is tightly associated with its pathogenesis. Based on *in vitro* studies, the cAMP-protein kinase A (PKA) pathway is a key regulator of *C. albicans* morphogenesis. Using an intravital imaging approach, we investigated the role of the cAMP-PKA pathway during infection. Consistent with their roles *in vitro*, the downstream effectors of the cAMP-PKA pathway Efg1 and Nrg1 function, respectively, as an activator and a repressor of *in vivo* filamentation. Surprisingly, strains lacking the adenylyl cyclase, *CYR1*, showed only slightly reduced filamentation *in vivo* despite being completely unable to filament in RPMI + 10% serum at 37°C. Consistent with these findings, deletion of the catalytic subunits of PKA (Tpk1 and Tpk2), either singly or in combination, generated strains that also filamented *in vivo* but not *in vitro*. *In vivo* transcription profiling of *C. albicans* isolated from both ear and kidney tissue showed that the expression of a set of 184 environmentally responsive genes correlated well with *in vitro* filamentation (R^2, 0.62 to 0.68) genes. This concordance suggests that the *in vivo* and *in vitro* transcriptional responses are similar but that the upstream regulatory mechanisms are distinct. As such, these data emphatically emphasize that *C. albicans* filamentation is a complex phenotype that occurs in different environments through an intricate network of distinct regulatory mechanisms.

IMPORTANCE The fungus *Candida albicans* causes a wide range of disease in humans from common diaper rash to life-threatening infections in patients with compromised immune systems. As such, the mechanisms for its ability to cause disease are of wide interest. An intensely studied virulence property of *C. albicans* is its ability to switch from a round yeast form to filament-like forms (hyphae and pseudohyphae). Surprisingly, we have found that a key signaling pathway that regulates this transition *in vitro*, the protein kinase A pathway, is not required for filamentation during infection of the host. Our work not only demonstrates that the regulation of filamentation depends upon the specific environment *C. albicans* inhabits but also underscores the importance of studying these mechanisms during infection.

KEYWORDS *Candida albicans*, fungal pathogenesis, NFAT transcription factors, protein kinase A, cyclic AMP, hyphae

Candida albicans is the most common human fungal pathogen and causes disease in both immunocompetent and immunocompromised patients (1). Accordingly, the mechanisms of *C. albicans* pathogenesis have been of broad and ongoing interest (2). One of the most intensively studied *C. albicans* virulence traits is its ability to transition between yeast and filamentous (hyphae and pseudohyphae) morphologies (3). All three morphotypes are observed in infected tissue by histology, and strains that are genetically "locked" as yeast or filaments have reduced ability to cause disease, indicating that the ability to transition between morphologies is important for pathogenesis (4).

Editor Judith Berman, Tel Aviv University

Address correspondence to Damian J. Krysan, damian-krysan@uiowa.edu.

The authors declare no conflict of interest.

This article is a direct contribution from Damian J. Krysan, a Fellow of the American Academy of Microbiology, who arranged for and secured reviews by Michael Lorenz, University of Texas Health Science Center, and Joseph Heitman, Duke University.

Received 24 March 2022
Accepted 25 March 2022
Published 27 April 2022

Consistent with its importance to *C. albicans* pathobiology, the genetic and molecular mechanisms of filamentation have been extensively studied, and a large set of genes positively and negatively affect the process (1, 5). Of the signaling pathways involved, the cAMP-protein kinase A (PKA) pathway (Fig. 1A) has been shown to regulate *in vitro* filamentation in response to a wide range of stimuli, including heat, carbon dioxide, and bacterial glycopeptides (6). Previous studies also support a model whereby the PKA pathway regulates filamentation through the direct phosphorylation/activation of Efg1 (7) and the indirect deactivation of Nrg1, a transcriptional repressor of filamentation (8). Efg1 is a bHLH type transcription factor that is required for filamentation in most but not all *in vitro* conditions (9). Efg1 contains multiple candidate PKA phosphorylation sites; mutation of one of these, threonine 206, to a nonphosphorylatable alanine (*efg1*^{T206A}) reduces filamentation in Spider and GlcNAc medium but not in the presence of serum (7). Overexpression of *EFG1* also partially suppresses the filamentation defect of a strain lacking one of the catalytic subunits of PKA (Tpk2). Nrg1 is a conserved transcriptional repressor that must be derepressed or degraded for filamentation to occur, and strains lacking *NRG1* are constituently filamentous (8). The regulation of *NRG1* expression/degradation has also been genetically linked to the PKA pathway. Although the role of the PKA-Efg1-Nrg1 axis has been well-established *in vitro*, its effect on filamentation during mammalian infection has not been studied directly.

Recently, we developed an intravital imaging approach to the morphological characterization of *C. albicans* in infected tissue by directly injecting fluorescently labeled *C. albicans* into the subepithelial/submucosal tissue of mouse ears (10, 11). The *C. albicans* infection cycle begins with the yeast penetrating through the mucosal/epithelial cells to the submucosal/stromal tissue from which it then gains access to the vasculature and disseminates (2). The ear model directly establishes infection within the stroma and thus recapitulates this intermediate step of the cycle (10, 11). In this way, the distribution of yeast and filamentous forms of the fungus during infection of a pathogenically relevant tissue can be quantitatively characterized.

As we reported previously (11), Efg1 is required for filamentation in this model in both reference strains and clinical isolates. Consequently, we were interested to determine if other components of the cAMP-PKA pathway (Fig. 1C) also regulated *in vivo* filamentation. To do so, a 1:1 mixture of NEON-labeled wild-type (WT) reference and an i-RFP-labeled homozygous deletion mutant was injected into the subdermal ear tissue of a DBA/2 mouse; 24 h postinfection, the mouse ear was imaged by confocal microscopy and the ratio of filamentous and yeast cells determined for WT and the mutant (see below for details). Consistent with our previous reported data (11), WT cells show a consistent percentage of filaments (80%) 24 h postinfection; this percentage is similar to that observed *in vitro* after cells are induced with RPMI + 10% serum at 37°C for 4 h (Fig. 1B). *In vitro*, deletion of *NRG1* leads to a constitutively hyphal strain (12, 13). Consistent with the *in vitro* phenotype, the *nrg1*ΔΔ mutant also formed an increased percentage of hyphal cells *in vivo* (Fig. 1B). Taken together with our previously reported results for the *efg1*ΔΔ mutant, these data indicate that the downstream transcriptional regulators of the PKA pathway carry out similar functions *in vitro* and *in vivo*.

In vitro, the adenylyl cyclase, *CYR1*, integrates hypha-inducing inputs from multiple stimuli and pathways to activate the PKA pathway by generating cAMP (Fig. 1A) (3, 6). Surprisingly, a strain lacking *CYR1* formed filaments *in vivo* nearly as well as WT (Fig. 1C), while no hyphae were formed *in vitro* (see Fig. S1A in the supplemental material), indicating that cAMP-independent pathways predominately regulate filamentation *in vivo*. Parrino et al. (14) and Min et al. (15) have described cAMP-independent filamentation *in vitro* based on the isolation of extragenic suppressors of the *cyr1*ΔΔ mutant that are able to filament *in vitro*. Characterization of these suppressors revealed that the suppression was due to loss of function mutations in *BCY1*, the gene that encodes the cAMP-responsive negative regulator of PKA (Fig. 1A). If this bypass mechanism were operative *in vivo*, then filamentation would still be dependent on the PKA kinase isoforms, *TPK1* and *TPK2*. As shown in Fig. 1D, deletion of neither PKA isoform reduces filamentation dramatically *in vivo* while in RPMI + 10% serum, both *tpk1*Δ and *tpk2*Δ mutants have modest defects (see Fig. S1B).

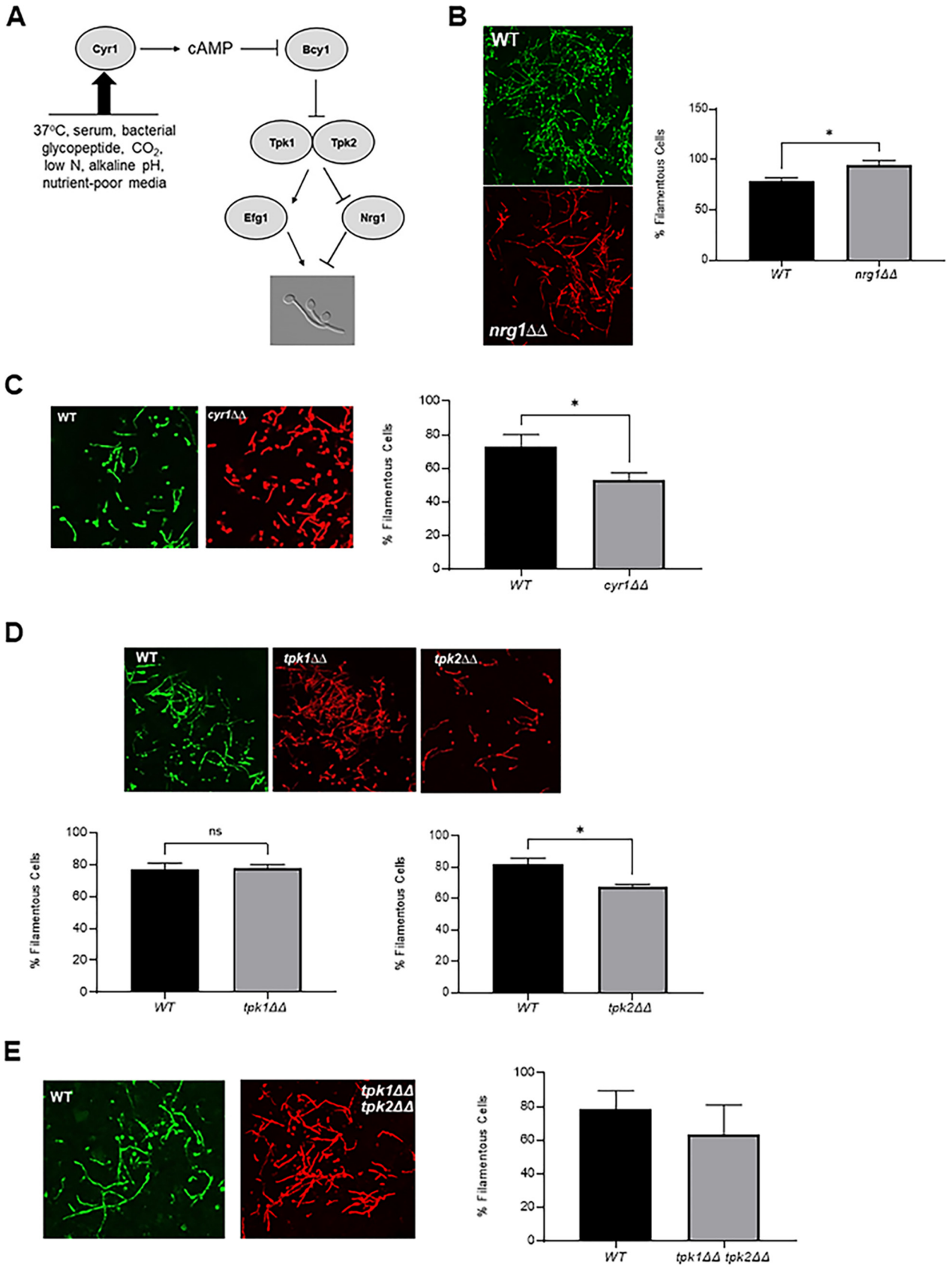

FIG 1 The cAMP-protein kinase A pathway is not required for *C. albicans* filamentation *in vivo*. (A) Simplified schematic of the cAMP-protein kinase A pathway and its *in vitro* inducers. (B to D) Images of WT (green) and the indicated mutant (red) visualized by confocal microscopy

(Continued on next page)

It remained possible that Tpk1 and Tpk2 have redundant roles during *in vivo* filamentation. Recently, strains lacking both Tpk1 and Tpk2 subunits have been generated and shown to be unable to filament *in vitro* (16). To test the Tpk1/2 dependence of *in vivo* filamentation, we constructed an iRFP-tagged *tpk1*ΔΔ *tpk2*ΔΔ mutant and confirmed that it was unable to filament *in vitro* (Fig. S1C). In contrast to *in vitro* conditions, and consistent with the results with the *cyr1*ΔΔ mutant, the *tpk1*ΔΔ *tpk2*ΔΔ double mutant forms filaments *in vivo* (Fig. 1E). Taken together, these data indicate that three of the key components of the cAMP-PKA pathway are largely dispensable for filamentation *in vivo*.

Since the transcriptional regulators of the canonical cAMP-PKA pathway retain their roles *in vitro* and *in vivo*, we predicted that the transcriptional responses during filamentation *in vitro* and *in vivo* would also be similar. To test this prediction, we compared the expression profile of our reference strain (SN425) during yeast phase growth (30°C, yeast peptone dextrose [YPD]) to *in vitro* induction with RPMI + 10% bovine calf serum (BCS) at 37°C and to cells isolated from two sites of *in vivo* filamentation (ear tissue and kidney tissue following disseminated infection). We used a NanoString probe set (185 genes) based on one previously used by Xu et al. (17) to profile *C. albicans* isolated from kidney organs following disseminated infection. This set contains environmentally responsive genes of which 25% are hyphae associated (for full list, see Table S1 in the supplemental material).

Cells were isolated after 4 h of induction, while the *in vivo* samples were collected at 24 h postinfection; the same time points used form morphological characterization. The absolute expression of the genes was significantly correlated for all three samples. The correlation between expression in the kidney and ear (Fig. 2A) was slightly stronger than either infection site with *in vitro* induction conditions (Fig. 2B and C). Although this is a small set of genes, the strong correlation in expression between *C. albicans* in the ear and the kidney supports the notion that filamentation in the ear is transcriptionally similar to the kidney and, although there are likely to be some differences, the two sites are reasonably comparable. The similarity of the transcriptional responses is further supported by the fact that very few genes are uniquely regulated in a single condition (Fig. 2D). Thus, the cAMP-PKA independence of *in vivo* filamentation cannot be explained by dramatic differences in the transcriptional responses and indicate that upstream regulators of the transcriptional responses are distinct between *in vitro* induction and *in vivo* infection of tissue.

These data have important implications for current models of *C. albicans* morphogenesis. First, many studies have shown that *in vitro* filamentation is largely cAMP-PKA dependent (3, 5, 6); our data indicate that, while the cAMP-PKA pathway does contribute to filamentation *in vivo*, cAMP-PKA-independent mechanisms appear to predominate. Second, the standard models of *C. albicans* filamentation posit that PKA directly phosphorylates Efg1 to mediate filamentation (7). *In vivo*, the discordance between the phenotypes of Efg1 and PKA pathway mutants indicates that Efg1 is independent of the cAMP-PKA pathway under these conditions. Third, the consistent roles of Efg1 and Nrg1 under the two conditions, along with the similarity of the transcriptional responses of *in vitro* and *in vivo* filamentation, indicate that distinct upstream regulatory pathways mediate a relatively conserved transcriptional response. It must be noted, however, that histological analyses indicate that Efg1 does not appear to be required for filamentation in the oral cavity and, thus, additional Efg1-independent pathways are also likely to be present (18, 19). Overall, these data and previously reported results emphatically emphasize that *C. albicans* filamentation is a complex phenotype that occurs in different environmental niches through an intricate network of distinct regulatory mechanisms.

Strains, cultivation conditions, and media. All *C. albicans* strains were constructed in the SN background (20) except for the *cyr1*ΔΔ mutant, which was generously provided by Jamie Konopka and was constructed in the BWP17 background (14, 15). The *nrg1*ΔΔ deletion

FIG 1 Legend (Continued)
visualized 24 h after coinoculation into the pinna of a DBA/2 mouse. The accompanying graphs show quantitation of the percent of filamentous cells using the scoring system described. The bars represent at least two independent replicates in which >100 cells were scored in multiple fields. The error bars indicate standard deviation, and asterisks indicate that WT and the mutant differ in a statistically significant amount (Student's *t* test, $P < 0.05$). (B) *nrg1*ΔΔ mutant. (C) *cyr1*ΔΔ mutant. (D) *tpk1*ΔΔ, *tpk2*ΔΔ, and *tpk1*ΔΔ *tpk2*ΔΔ mutants.

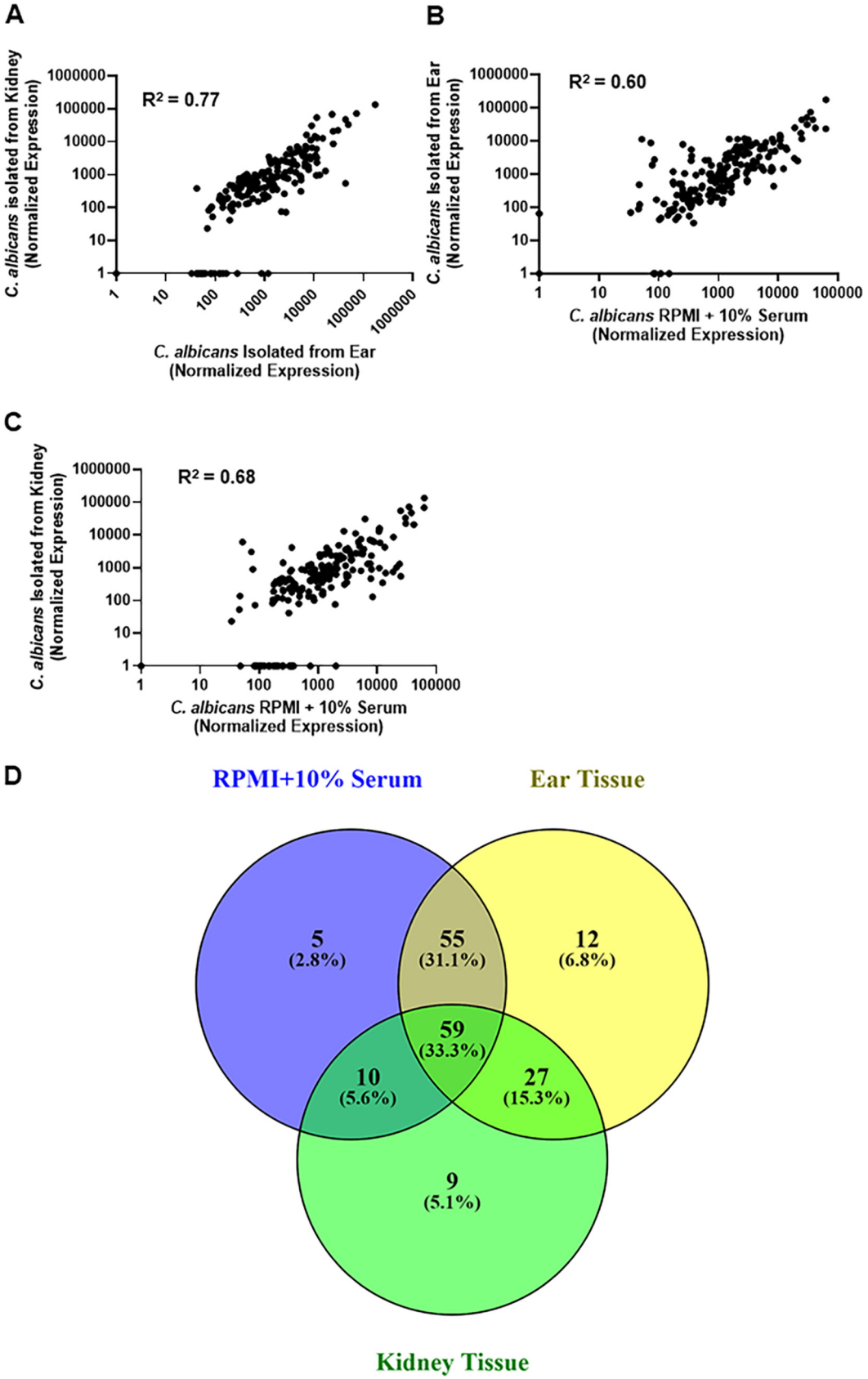

FIG 2 The expression of a set of 185 environmentally responsive genes is similar between *in vitro* hyphae induction and infection of either mouse ear or kidney. The normalized RNA counts measured by NanoString nCounter for *C. albicans*

(Continued on next page)

was from the collection of Homann et al. (20), obtained from the Fungal Genetics Stock Center, and confirmed by phenotype and genotype. The *tpk1*ΔΔ and *tpk2*ΔΔ mutants were generated using standard CRISPR-based methods. The *tpk1*ΔΔ *tpk2*ΔΔ double mutants were constructed using the recently described CRIME methodology (21). Briefly, both copies of *TPK2* were knocked out by cotransforming the recipient strain with a split *LEU2* cassette with *TPK2* homology at both ends and two *TPK2* gene targeting guide RNAs (oligonucleotides used to construct the deletion mutants are listed in Table S2 in the supplemental material). In the resulting *tpk2*ΔΔ mutants, the *LEU2* cassette was recycled by cotransformation of the mutant strain with an *LEU2* and *ARG4*-targeting constructs along with an *ARG4* cassette, which served as a selection marker. The resulting *tpk2*ΔΔ mutants with excised *LEU2* cassette were then used to construct double *tpk1*ΔΔ *tpk2*ΔΔ knockout mutants using the same approach as above. Correct integration and absence of the targeted open reading frames (ORFs) was confirmed by PCR analysis.

Reference strains SN and BWP17 were labeled by transforming with pENO1-NEON-NAT1, while mutant strains were transformed with pENO1-iRFP-NAT1 as previously described. All *Candida albicans* strains were precultured overnight in yeast peptone dextrose (YPD) medium at 30°C. Standard recipes were used to prepare media (18). RPMI medium was purchased and supplemented with bovine serum (10%, vol/vol). The yeast phase cells for NanoString analysis were inoculated into fresh YPD medium and incubated for 4 h to achieve mid-log phase. For *in vitro* hyphae induction, *C. albicans* strains were incubated overnight in YPD at 30°C, harvested, and diluted into RPMI + 10% serum at a 1:50 ratio and incubated at 37°C for 4 h. Cells were fixed with formalin, collected, and examined by light microscopy.

Intravital imaging and scoring. The inoculation and imaging were carried out exactly as described in reference 11. Filamentous cells had identifiable mother cells, and the filamentous projection was at least twice the length of the mother cell body. Yeast cells were round and/or budded cells. Filamentous cells were confirmed by manually following the hyphal projection through each Z stack (30 stacks). Yeast cells were further required not to project through multiple Z stacks. At least 100 cells in multiple fields were scored; experiments were performed in duplicate or triplicate using independent isolates of strains. Statistical significance was determined by the unpaired Student's *t* test. The data sets did not show a detectable difference from normality using the Shapiro-Wilk test ($P > 0.05$). Statistical tests were performed using GraphPad Prism software.

***In vitro* and *in vivo* NanoString analysis.** For *in vitro* RNA extraction, three independent cultures were grown overnight in YPD at 30°C, harvested, and diluted into RPMI + 10% serum at a 1:50 ratio and incubated at 37°C for 4 h. Cells were collected and centrifuged for 2 min at 11,000 rpm at room temperature (RT), and RNA was extracted from the pellet according to the manufacturer protocol (MasterPure Yeast RNA purification kit, catalog number MPY03100). Extraction of RNA from mouse tissue was performed as reported by Xu et al. with some modification (17). Briefly, to extract RNA from the mouse ears, the following procedure was used. After 24 h postinjection, mice were euthanized following the protocol approved by the University of Iowa IACUC. The *C. albicans*-infected mouse ear was removed and directly placed in the ice-cold RNAlater solution, and then the ear was transferred to the mortar and flash frozen with liquid nitrogen. Further samples were ground to a fine powder, which was transferred to a 5-mL centrifuge tube, and 1 mL of ice-cold TRIzol was added. The samples were placed on a rocker at RT for 15 min and then centrifuged at 10,000 rpm at 4°C for 10 min to remove the debris. Cleared TRIzol was transferred to a 1.5-mL Eppendorf tube, and 200 μL of RNase free chloroform was added to each sample. Tubes were shaken vigorously for 15 s and kept at RT for 5 min followed by centrifuge at 12,000 rpm for 15 min

FIG 2 Legend (Continued)
cells induced to form hyphae *in vitro* (RPMI + 10% serum, 37°C, 4 h), isolated from infected ear and isolated from infected kidney, were plotted and analyzed for correlation using Pearson's coefficient. All correlations are statistically significant. (A) Kidney versus ear. (B) Ear versus *in vitro*. (C) Kidney versus *in vitro*. (D) Venn diagram for comparing the overlap of differentially expressed genes (2-fold change, statistically significant by Student's *t* test, $P < 0.05$) between the three conditions. Data for the plots are summarized in Table S1 in the supplemental material.

at 4°C. The cleared aqueous layer was then transferred to a new 1.5-mL tube, and RNA was further extracted according the Qiagen RNeasy kit protocol.

RNA (40 ng for *in vitro* and 1.4 μg for *in vivo*) was added to a NanoString CodeSet mix (see Table S1) and incubated at 65°C for 18 h. After hybridization reaction, samples were proceeded to nCounter prep station, and samples were scanned on an nCounter digital analyzer. nCounter .RCC files for each sample were imported into nSolver software to evaluate the quality control metrics. Using the negative control probes, the background values were first assessed. The mean plus standard deviation of negative control probes value was defined and used as a background threshold, and this value is subtracted from the raw counts. The background subtracted total raw RNA counts were normalized against the highest total counts from the biological triplicates. The statistical significance of changes in counts was determined by two-tailed Student's *t* test ($P < 0.05$). The expression data are summarized in Table S1. Probes that were below background were set to a value of 1 to allow statistical analysis. The raw counts, normalized counts, and statistical analyses are also provided in Table S1.

SUPPLEMENTAL MATERIAL

Supplemental material is available online only.

FIG S1, TIF file, 0.5 MB.

TABLE S1, XLSX file, 0.1 MB.

TABLE S2, PDF file, 0.1 MB.

ACKNOWLEDGMENTS

This work was supported by NIH grants R01AI133409 (D.J.K.) and R21AI157341 (D.J.K.).

We thank Jamie Konopka (Stony-Brook), Aaron Mitchell (Georgia), and Scott Filler (UCLA) for reading early versions of the manuscript and helpful suggestions, Jamie Konopka for providing strains, and Robert Wheeler (Maine) for providing plasmids.

Conceptualization, Damian J. Krysan, Melanie Wellington; Formal analysis, Rohan W. Wakade, Juraj Kramara, Melanie Wellington, and Damian J. Krysan; Investigation, Rohan S. Wakade, Juraj Kramara; Methodology, Rohan S. Wakade, Juraj Kramara; Supervision, Melanie Wellington, Damian J. Krysan; Writing-original draft, Damian J. Krysan; Writing-review and editing, Damian J. Krysan.

REFERENCES

1. McCarty TP, Pappas PG. 2016. Invasive candidiasis. Infect Dis Clin North Am 30:103–124. https://doi.org/10.1016/j.idc.2015.10.013.
2. Lopes PJ, Lionakis MS. 2022. Pathogenesis and virulence of *Candida albicans*. Virulence 13:89–121. https://doi.org/10.1080/21505594.2021.2019950.
3. Sudbery PE. 2011. Growth of *Candida albicans* hyphae. Nat Rev Microbiol 9:737–748. https://doi.org/10.1038/nrmicro2636.
4. Saville SP, Lazzell AL, Monteagudo C, Lopez-Ribot JL. 2003. Engineered control of cell morphology in vivo reveals distinct roles for yeast and filamentous forms of *Candida albicans* during infection. Eukaryot Cell 2:1053–1060. https://doi.org/10.1128/EC.2.5.1053-1060.2003.
5. Arkowitz RA, Bassilana M. 2019. Recent advances in understanding *Candida albicans* growth. F1000Res 8:F1000 Faculty Rev-700. https://doi.org/10.12688/f1000research.18546.1.
6. Huang G, Huang Q, Wei Y, Wang Y, Du H. 2019. Multiple roles and diverse regulation of the RAS/cAMP/protein kinase A pathway in *Candida albicans*. Mol Microbiol 111:6–16. https://doi.org/10.1111/mmi.14148.
7. Bockmühl DP, Ernst JF. 2001. A potential phosphorylation site for an A-type kinase in the Efg1 regulator protein contributes to hyphal morphogenesis of Candida albicans. Genetics 157:1523–1530. https://doi.org/10.1093/genetics/157.4.1523.
8. Lu Y, Su C, Liu H. 2014. *Candida albicans* hyphal initiation and elongation. Trends Microbiol 22:707–714. https://doi.org/10.1016/j.tim.2014.09.001.
9. Villa S, Hamideh M, Weinstock A, Qasim MN, Hazbun TR, Sellam A, Hernday AD, Thangamani S. 2020. Transcriptional control of hyphal morphogenesis in *Candida albicans*. FEMS Yeast Res 20:foaa005. https://doi.org/10.1093/femsyr/foaa005.
10. Mitra S, Dolan K, Foster TH, Wellington M. 2010. Imaging morphogenesis of *Candida albicans* during infection in a live animal. J Biomed Opt 15:e010504. https://doi.org/10.1117/1.3290243.
11. Wakade RS, Huang M, Mitchell AP, Wellington M, Krysan DJ. 2021. Intravital imaging of *Candida albicans* identifies differential in vitro and in vivo filamentation phenotypes for transcription factor deletion mutants. mSphere 6:e00436-21. https://doi.org/10.1128/mSphere.00436-21.
12. Braun BR, Kadosh D, Johnson AD. 2001. *NRG1*, a repressor of filamentous growth in *C. albicans*, is down regulated during filament induction. EMBO J 20:4753–4761. https://doi.org/10.1093/emboj/20.17.4753.
13. Murad AM, Leng P, Straffon M, Wishart J, Macaskill S, MacCallum D, Schnell N, Talibi D, Marechal D, Tekaia F, d'Enfert C, Gaillardin C, Odds FC, Brown AJ. 2001. *NRG1* represses yeast-hypha morphogenesis and hypha-specific gene expression in *Candida albicans*. EMBO J 20:4742–4752. https://doi.org/10.1093/emboj/20.17.4742.
14. Parrino SM, Si H, Naseem S, Groudan K, Gardin J, Konopka JB. 2017. cAMP-independent signal pathways stimulate hyphal morphogenesis in *Candida albicans*. Mol Microbiol 103:764–779. https://doi.org/10.1111/mmi.13588.
15. Min K, Jannace TF, Si H, Veeramah KR, Haley JD, Konopka JB. 2021. Integrative multi-omics profiling reveals cAMP-independent mechanisms regulating hyphal morphogenesis in *Candida albicans*. PLoS Pathog 17:e1009861. https://doi.org/10.1371/journal.ppat.1009861.
16. Cao C, Wu M, Bing J, Tao L, Ding X, Liu X, Huang G. 2017. Global regulatory roles of the cAMP/PKA pathway revealed by phenotypic, transcriptomic and phosphoproteomic analyses in a null mutant of the PKA catalytic subunit in *Candida albicans*. Mol Microbiol 105:46–64. https://doi.org/10.1111/mmi.13681.
17. Xu W, Solis NV, Ehrlich RL, Woolford CA, Filler SG, Mitchell AP. 2015. Activation and alliance of regulatory pathways in *C. albicans* during mammalian infection. PLoS Biol 13:e1002076. https://doi.org/10.1371/journal.pbio.1002076.
18. Riggle PJ, Andrutis KA, Chen X, Tzipori SR, Kumamoto CA. 1999. Invasive lesions containing filamentous forms produced by a *Candida albicans*

mutant that is defective in filamentous growth in culture. Infect Immun 67:3649–3652. https://doi.org/10.1128/IAI.67.7.3649-3652.1999.
19. Solis NV, Wakade RS, Glazier VE, Ollinger TL, Wellington M, Mitchell AP, Filler SG, Krysan DJ. 2022. Systematic genetic interaction analysis identifies a transcription factor circuit required for oropharyngeal candidiasis. mBio 13:e03447-21. https://doi.org/10.1128/mbio.03447-21.
20. Homann OR, Dea J, Noble SM, Johnson AD. 2009. A phenotypic profile of the *Candida albicans* regulatory network. PLoS Genet 5:e1000783. https://doi.org/10.1371/journal.pgen.1000783.
21. Huang MY, Mitchell AP. 2017. Marker recycling in *Candida albicans* through CRISPR-Cas9-induced marker excision. mSphere 2:e00050-17. https://doi.org/10.1128/mSphere.00050-17.